Progress In Electromagnetics Research M, Vol. 119, 75–88, 2023

Global Optimization for Extinction Curve Reconstruction in Inverse Electromagnetic Scattering of Multiparticle Aggregates

Ying Li Thong and Tiem Leong Yoon*

Abstract—Generalized Mie theory provides a theoretical solution to the extinction cross-section curve of an electromagnetic scattering event with a multiparticle aggregate, given the configurational information of the constituent particles. However, deducing the configuration of the aggregate from the extinction cross-section curve is a nontrivial inverse problem that can be cast as a global optimization problem. To address this challenge, we propose a computational scheme that combines global optimization search algorithms with a calculator known as the Generalized Multiparticle Mie-solution. The scheme is tested using mock scattering cross-section curves based on randomly generated aggregate configurations. The scheme successfully reproduces the scattering curve by minimizing the discrepancy between the two scattering curves. However, the ground-truth configuration is not reproduced, as initially expected. This is due to the inability of the global optimization algorithm scheme used in the present work to correctly locate the global minimum in the high-dimensional parameter space. Nonetheless, the partial success of the proposed scheme to reconstruct the mock curves provides an instructive experience for future attempts to solve the inverse electromagnetic scattering problem by fine-tuning the present approach.

1. INTRODUCTION

The scattering of electromagnetic (EM) radiation (such as in a microwave scattering experiment) with an aggregate made up of spherical particles is a complicated process that could be modelled from first principles within the framework of Maxwell's equations. The solution to the general case of multiparticle scattering for an arbitrary aggregate made up of spherical particles is referred to as the generalized Mie theories (a.k.a. generalized Lorenz-Mie theories [1]). Generalized Mie theories provide a theoretical solution to the optical responses of an EM scattering event with a multiparticle aggregate of nano- or microscopic scales, such as the scatter, extinction, and absorption cross-section curves at a wavelength and scattering angle. The simplest solution to this problem was proposed by Mie in 1908 for the simplest case of a homogeneous sphere [2]. There are many rigorous models adopting different theoretical approaches and at different levels of approximation to solve such a complex calculation in EM scattering, e.g., [3–6].

The generalized multiparticle Mie-solution (GMM) [7–13] is an extension of Mie solution from a single particle to the multiparticle case that provides an analytical far-field solution to electromagnetic scattering by an aggregate of spheres in a fixed orientation. GMM was implemented as a freely downloadable Fortran package by Yu-lin Xu (https://scattport.org/files/xu/codes.htm, assessed on 15 Dec. 2021). It can compute the optical responses of an EM scattering event with a multiparticle aggregate, such as the extinction and absorption cross-sections of the scattered EM radiation as a function of scattering angle at a fixed wavelength. The aggregate is assumed to be made of nonintersecting homogeneous spheres embedded in a vacuum surrounding. GMM has been shown

Received 26 May 2023, Accepted 25 September 2023, Scheduled 24 September 2023
* Corresponding author: Tiem Leong Yoon (tlyoon@usm.my).
The authors are with the School of Physics, Universiti Sains Malaysia, 11800 USM, Penang, Malaysia.

to provide impressive agreement with experimental results as compared with the Mie theory and geometrical optics results [7]. The input information required by the GMM code includes the spatial coordinates, common radius, both the real and complex refractive indices of each constituent particle in the multi-particle aggregate. EM responses, such as the extinction cross-section σ_{ext}, are returned as outputs from a scattering event between an incident EM radiation and the aggregate.

Computationally, the GMM program can calculate the optical responses of an aggregate given the configurational information of the constituent particles, such as the number, size, coordinates, and common refractive indices. However, deducing the configuration of an aggregate from experimental curves of optical responses is a highly nontrivial task, due to not only the immense computational complexity involved but also the possible issues of non-uniqueness of the solutions. Examples of computational schemes for performing this task can be found in the literature, such as those referenced in [14]. The authors in [14] proposed an efficient numerical approach based on machine learning and evolutionary algorithms to retrieve particle size distribution from bulk optical properties. This problem is usually computationally expensive, but the authors overcame this issue by accelerating the calculation of bulk optical properties through machine learning. They first used Mie scattering theory to solve the forward scattering by particles assuming spherical particles, and then approximated it using machine learning. The particle swarm optimization algorithm was applied to optimize the particle size distribution parameters by minimizing the deviation between the target and simulated bulk optical properties. Their approach was able to accurately predict the scattering efficiency for a specific size distribution in approximately 0.5 μs at a light computational cost.

Deducing the information of the aggregate configuration from the extinction cross-section curve is essentially a specific type of electromagnetic inverse scattering problem, which can be formulated as a global optimization problem. The main purpose of this article is to propose a computational scheme that can solve the electromagnetic inverse scattering problem. The problem to solve is a computational one, involving the integration of two independent ingredients: the generalized Mie theories and a global optimizer (GO). The generalized Mie theories take care of the physics governing the electromagnetic scattering process, while the global optimizer handles the computational optimization aspects of the problem. The proposed scheme is a computational implementation that integrates a global optimizer to search for solutions in the electromagnetic inverse scattering system in a high-dimensional configurational space of the aggregates. This was considered a daunting task before the advent of genetic algorithms for global optimization. Retrieving the configurational information of a multi-particle aggregate from experimentally measured optical-response curves is of practical significance for realistic applications. The computational scheme proposed in this work should be appreciated as a computational innovation that makes use of well-established global optimization algorithms and theoretical theories.

2. METHODOLOGY

Conceptually, the computation of the electromagnetic inverse scattering problem as proposed in the present scheme involves two conceptually distinct steps: curve reconstruction and comparison with ground-truth configuration.

2.1. The Overall Conceptual Strategy

The first step, known as curve reconstruction, involves developing a working procedure to reproduce an extinction cross-section curve (as a function of wavelength λ) from a random initial configuration. This was achieved by coupling the GMM code with a global optimizer. The configurations obtained at the end of the curve reconstruction process are expected to reproduce the given extinction cross-section curve when being used as input to the GMM code. These configurations are denoted as the 'optimized' configurations for easy reference. However, it is important to note that the optimized configurations are conceptually distinct from the 'ground-truth' configuration that originally produced the given extinction cross-section curve. In a real-life scenario, the 'ground-truth' configuration and the extinction cross-section curve are typically measured or obtained experimentally. The 'ground-truth' configuration is known to be responsible for giving rise to the consequential extinction cross-section curve via some form of theoretical principles such as generalized Mie theories. However, for the purpose of demonstrating the

proof of a working principle, the 'ground-truth' configurations were generated randomly in this study. To mimic experimentally measured extinction cross-section curves, these 'ground-truth' configurations were fed into the GMM code. The resulting extinction cross-section curves are denoted by the superscripted symbol $\sigma_{\text{ext}}^{\text{mock}}(\lambda)$, which indicates an extinction cross-section curve generated via the aforementioned procedure (dubbed 'mock data generation'). We shall refer to $\sigma_{\text{ext}}^{\text{mock}}(\lambda)$ as the 'mock experimental curve'. The details of the mock data generation procedure will be explained in the later part of this manuscript.

The second step, known as 'comparison with ground-truth configuration', involves comparing the optimized configurations (obtained from the curve reconstruction step) to the 'ground-truth' configurations. The curve reconstruction computation takes in the $\sigma_{\text{ext}}^{\text{mock}}(\lambda)$ curve as input but remains blind with respect to the 'ground-truth' configuration. As such, the 'optimized' and 'ground-truth' configurations are two independent sets of configurations. If the scheme proposed in the present proof of principle works, these two independent configurations should coincide with each other.

The solution to the electromagnetic inverse scattering problem proposed by the present scheme is deemed successful if it passes both the curve reconstruction and comparison with ground-truth configuration steps for any arbitrary $\sigma_{\text{ext}}^{\text{mock}}(\lambda)$ curve. The conceptual flowchart of the computational procedure to solve the specific type of electromagnetic inverse scattering problem proposed in this work is elaborated in Figure 1.

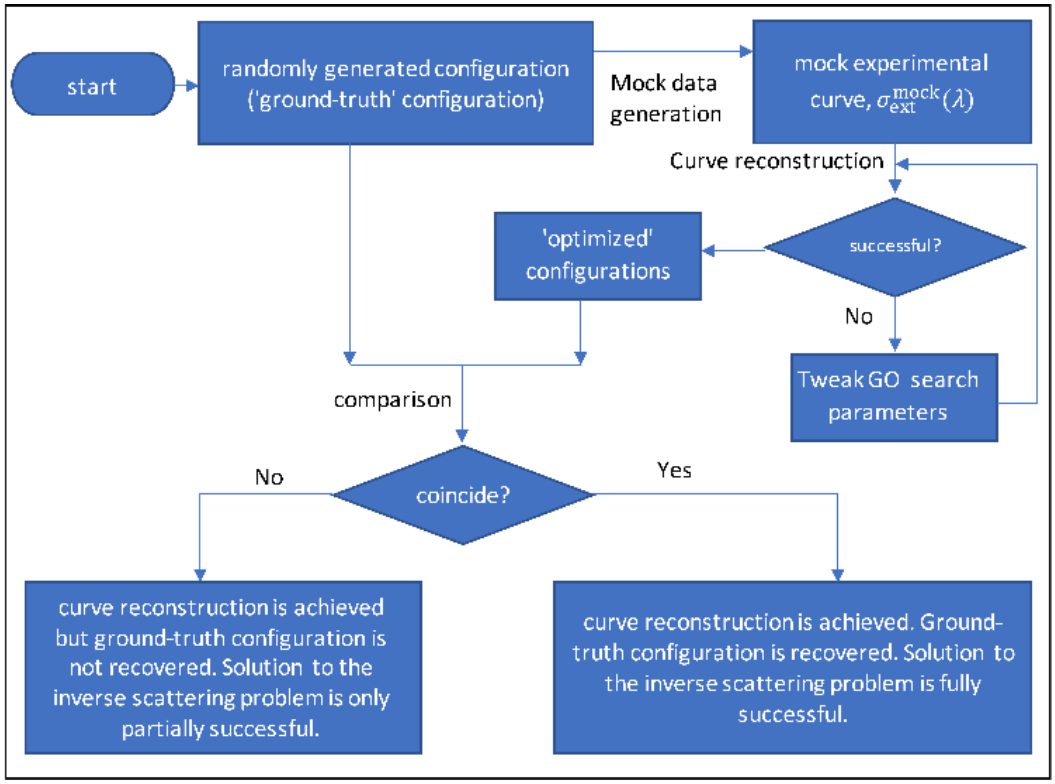

Figure 1. The conceptual flowchart of the computational procedure to solve the specific type of electromagnetic inverse scattering problem proposed in this paper.

2.2. The Global Optimizer

The computational tool in the curve reconstruction step comprises two integral components: 'global optimizer' and 'calculator'. The GMM code plays the role of the calculator. The function of the GO is to guide the process of configuration generation such that when they are fed into the GMM

calculator, they produce an extinction cross-section curve $\sigma_{\text{ext}}(\lambda)$ that progressively converges to a given $\sigma_{\text{ext}}^{\text{mock}}(\lambda)$. One of the global optimizers that can do this is Genetic Algorithm [15, 16], a stochastic optimization technique inspired by natural selection. Essentially, the genetic algorithm operates by creating a population of configurations that are iteratively evolved over multiple generations to maximize the objective function, which measures the deviation between the $\sigma_{\text{ext}}(\lambda)$ curve obtained from the GMM calculator and the target $\sigma_{\text{ext}}^{\text{mock}}(\lambda)$ curve. The evolution of the population involves the application of genetic operators to create new configurations that have a higher probability of producing a better fitness value. The fittest configurations from each generation are selected to form the population of the next generation, and this process is repeated until convergence to the desired target is achieved.

In the present study, the global optimization algorithms were adopted from the well-known optimization package Dakota [17]. The optimization class capability in Dakota Optimization solvers provides a convenient application interface (API) for coupling with an external 'simulator' (in Dakota terminology), which is the GMM calculator in the present context. Dakota Optimization solvers provide a selection of derivative-free global optimization algorithms that are suitable for the inverse scattering problem being dealt with here, including the multiobjective genetic algorithm (MOGA) and coliny_pattern_search.

MOGA [18] is a stochastic optimization algorithm that is based on the principles of natural selection. It works by generating a population of candidate solutions, and then iteratively improving the population by selecting the best solutions and recombining them to form new solutions. The MOGA in the Dakota package [19] is provided by the JEGA library [20]. The MOGA in Dakota is a real-coded genetic algorithm that inherits the strengths of the well-known and well-tested NSGA-II algorithm. It adds additional features, such as Pareto dominance sorting and diversity maintenance to make it suitable for a wide variety of optimization problems. Pareto dominance sorting ensures that the best solutions are always at the top of the population, while diversity maintenance helps to prevent the algorithm from converging to a single solution and finding a wider range of good solutions.

The keywords that control in the MOGA in Dakota include fitness_type, replacement_type, convergence_type, max_iterations, max_function_evaluations, population_size, initialization_type, crossover_type, mutation_type and convergence_tolerance. To deploy the MOGA in the Dakota package for solving our global optimization problem, the values to these parameters need to be set. A typical list of MOGA parameters adopted in our calculations in the present work is as listed in Table 1. However, the parameters used are by no means rigidly fixed. The exact values and child keyword for the keyword types may have to be tuned based on a case-by-case basis to achieve convergence.

Table 1. Typical values of parameters used in the MOGA.

Keyword type	**Child keyword**	**Value**
fitness_type	merit_function	-
replacement_type	elitist	-
convergence_type	average_fitness_tracker	percent_change=0.1 num_generations=60
max_iterations		60000
max_function_evaluations		60000
population_size		100
initialization_type	unique_random	
crossover_type	shuffle_random	num_parents=20 num_offspring=15 crossover_rate=15.0
mutation_type	replace_uniform	mutation_rate=0.1
convergence_tolerance	-	$1{\cdot}e^{-5}$
final_solutions	-	1

In Table 1, the three keywords fitness_type, replacement_type, and convergence_type control the evaluation of the new population in the MOGA in Dakota.

- The fitness_type keyword specifies the type of fitness function to use. merit_function is a scalar function that evaluates the quality of a solution. The best solution is the one with the highest merit_function value.
- The replacement_type keyword specifies the type of replacement strategy to use. The elitist strategy only replaces the worst solutions in the population with new solutions. This ensures that the best solutions are always preserved in the population.
- The convergence_type keyword specifies the convergence criteria to use. average_fitness_tracker monitors the average fitness of the population over time. The algorithm will terminate if the average fitness does not change by more than the value specified by percent_change and num_generations.

The coliny_pattern_search is a stochastic optimization algorithm that is based on the principles of pattern search. Pattern search is a deterministic optimization algorithm that works by iteratively searching for the best solution in a neighborhood of the current solution. The algorithm extends pattern search by introducing a stochastic element into the search process. This stochastic element allows the algorithm to escape from local minima and find better solutions.

The above two algorithms offered in the Dakota package had been adopted in a hybrid mode. To perform a hybrid search, we executed the MOGA for global optimization followed by the coliny_pattern_search algorithm for local minimization search. This two-step approach is a recommended method for performing global optimization in the Dakota manual (see Section 14.2 in the Dakota manual [17]). As a technical note, the MOGA in the Dakota package can also be employed for multiple objective global optimization. However, in our work, it was utilized for single objective global optimization by setting the number of objective functions to one (i.e., by setting the keyword type in the Dakota input script final_solutions to an integer 1), which is essentially equivalent to the so-called single-objective genetic algorithm (SOGA).

2.3. Procedure of Curve Reconstruction

We first downloaded the source code of GMM and compiled it to produce an executable named 'gmm01f'. This was the GMM calculator. It was then stitched into the Dakota package via the provided API by following a step-by-step procedure described in the Dakota user manual [17]. The Dakota-GMM API was successfully tested and assembled, and subsequently deployed on a Linux-based server to search for an unknown configuration that produces a scattering curve $\sigma_{\text{ext}}(\lambda)$ with a globally minimized discrepancy against the mock experimental curve $\sigma_{\text{ext}}^{\text{mock}}(\lambda)$.

The objective function, also known as the fitness function, was the mean square error (MSE) σ^2, defined as follows:

$$\sigma^2 = \frac{1}{N_\lambda} \sum_{i=0}^{N_\lambda} \left[\sigma_{\text{ext}}(\lambda_i) - \sigma_{\text{ext}}^{\text{mock}}(\lambda_i) \right]^2. \tag{1}$$

Here, λ_i, $i \in \{0, 1, ..., N_\lambda\}$ are the N_λ discrete values at which the wavelength λ in $\sigma_{\text{ext}}(\lambda)$ was sampled. The value of σ^2 quantifies the discrepancy between the scattering curves produced by Dakota-GMM and the mock experimental data. Both of the $\sigma_{\text{ext}}^{\text{mock}}(\lambda)$ and any intermediate $\sigma_{\text{ext}}(\lambda)$ curves produced by the GMM calculator were normalized as $\sum_{i=0}^{N_\lambda} \sigma_{\text{ext}}(\lambda_i) = \sum_{i=0}^{N_\lambda} \sigma_{\text{ext}}^{\text{mock}}(\lambda) = 1$.

The GMM calculator requires a set of numerical inputs to produce an output $\sigma_{\text{ext}}(\lambda)$. These inputs include the $3N$ spatial coordinates of the constituent particles $\{x_i, y_i, z_i\}$, where $i \in \{1, 2, ..., N\}$, with N being the number of particles making up the aggregate; r, n, κ are the common radius, real and imaginary refractive indices of the constituent particles, respectively. From a numerical perspective, σ^2 is a function of a set of variables $\{x_i, y_i, z_i; r, n, \kappa, N\}$, where $i \in \{1, 2, ..., N\}$, such that $\sigma^2 = \sigma^2(\{x_i, y_i, z_i; r, n, \kappa, N\})$. The total number of independent free variables in σ^2 is $3N + 4$. Given the set of variables $\{x_i, y_i, z_i; r, n, \kappa, N\}$, the GMM calculator will produce a list of output optical responses, one of which is $\sigma_{\text{ext}}(\lambda)$, based on the solution scheme encoded into GMM for the generalized Mie theories. In the most general scenario, Dakota performs a global minimum search for σ^2 in the $(3N + 4)$-dimensional parameter space. However, to simplify the establishment of the working principle

proposed in this work, r, n, κ and N were treated as known parameters and not treated as unknown variables for global minimization. This reduced the parameter space to a $3N$-dimensional space, such that $\sigma^2 = \sigma^2(\{x_i, y_i, z_i\})$ where $i \in \{1, 2, ..., N\}$.

In an iterative loop, the Dakota derivative-free global optimization algorithm generated a random configuration set $\{x_1, y_1, z_1; x_2, y_2, z_2; ...; x_N, y_N, z_N\}$ to feed into the GMM calculator. Note that the trial configurations, $\{x_i, y_i, z_i\}$, $i \in N$, play the role of 'chromosome' in genetic algorithm (GA). The objective function, i.e., the trial extinction cross-section curve $\sigma_{\text{ext}}(\lambda)$ in Eq. (1), was calculated by the GMM calculator based on these 'chromosomes'. The resultant σ^2 was fed back into Dakota. Taking the hint from the feedback σ^2 value, the global optimization algorithm would generate an improved set of configuration $\{x_1, y_1, z_1; x_2, y_2, z_2; ...; x_N, y_N, z_N\}'$ based on the prescribed algorithm built into the global optimizer. As the iteration was looped, the predicted curve by GMM, $\sigma_{\text{ext}}(\lambda)$, progressively converged into the mock curve $\sigma_{\text{ext}}^{\text{mock}}(\lambda)$ due to the operation of global minimization, in which the value of σ^2 was minimized as a function of the $3N$ coordinate variables. As a technical note, the GMM code did not always return a converged output, i.e., a $\sigma_{\text{ext}}(\lambda)$ curve, for any arbitrary set of input, $\{x_i, y_i, z_i; r, n, \kappa, N\}$. This situation occurred, for example, when the constituent particles overlapped, or some physical constraints built into the GMM code were violated. When the GO generated a configuration that was not convergent upon feeding it into the GMM calculator, a high value of $\sigma^2 = 99999$ was artificially assigned. This represented a high penalty to the objective function, hence reminding the GO such a configuration was unfavorable and should be avoided in the following rounds of iteration.

The mock data generation procedure, alluded to in earlier paragraphs, generated a collection of random configurations $\{x_i, y_i, z_i\}_{\text{ground-truth}}$ and the corresponding $\sigma_{\text{ext}}^{\text{mock}}(\lambda)$ curves. $\sigma_{\text{ext}}^{\text{mock}}(\lambda)$ were generated based on randomly generated configurations using the GMM calculator to mimic experimental data. A good collection of $\sigma_{\text{ext}}^{\text{mock}}(\lambda)$ samples with a variety of trends and features was required to establish the proof of principle that the Dakota-GMM scheme could always attain a successful curve reproduction, and not restricted to only featureless, approximately flat $\sigma_{\text{ext}}^{\text{mock}}(\lambda)$. To this end, a Python script was written to generate a collection of random configurations $\{x_i, y_i, z_i\}_{\text{ground-truth}}$, $i \in \{1, 2, ..., N\}$ where N is the number of particles and r the value of the common radius of the constituent particles (in nm), while n, κ were arbitrarily selected from the range of 1.05–10.5. $\{x_i, y_i, z_i\}_{\text{ground-truth}}$ were generated by randomly chosen from the lattice sites of a hexagonal close-packed (HCP) system such that each particle shared at least one closest neighbor in contact and no individual particle was detached from the bulk. A $\sigma_{\text{ext}}^{\text{mock}}(\lambda)$ curve generated via the mock data generation procedure was characterized by a set of parameter values $\{r, n, \kappa, N\}$. The apparently unphysical values selected for n and κ were not meant to bear any physical significance but merely a convenient choice for producing a collection of $\sigma_{\text{ext}}^{\text{mock}}(\lambda)$ curves with more varying trends and features. It was found that the $\sigma_{\text{ext}}^{\text{mock}}(\lambda)$ curves produced by the GMM calculator were rather flat, featureless, and insensitive for most of the values of r, n, and N, and for small values of κ despite the randomness in the $\{x_i, y_i, z_i\}_{\text{ground-truth}}$ configuration. The feature in the trend of $\sigma_{\text{ext}}^{\text{mock}}(\lambda)$ curves in different $\{x_i, y_i, z_i\}_{\text{ground-truth}}$ configurations became more varied (in the sense that they deviate away from an approximately flat, featureless straight line) for large (despite unphysical) value of κ. Selected samples of $\sigma_{\text{ext}}^{\text{mock}}(\lambda)$ curves are as displayed in plot (a) in Figs. 3–5 in the Results and Discussion section.

To initiate a global minimization search, the Dakota code required a random set of coordinates $\{x_i, y_i, z_i\}$. These initial guesses were randomly generated within an interval $-L/2 \leq x_i, y_i, z_i \leq L/2$, where $L = N_b \cdot (2r \cdot N^{\frac{1}{3}})$, N_b a positive integer suitably set as $N_b = 3$. Such a choice of L, which is a function of $L = L(r, N)$, corresponds to a square box of side L that could comfortably accommodate an aggregate made up of N constituent particles with a common radius r, assuming that the particles did not line up bumper-to-bumper forming a straight chain (if this were the case the $\frac{L}{2} \times \frac{L}{2}$ square box would not be able to contain the aggregate). For example, for $N = 14$, $r = 100\,\text{nm}$, the upper and lower limits were $\pm L/2 = \pm 723\,\text{nm}$. In the Dakota input script, $[-L/2, L/2]$ were set as the lower and upper limits of $\{x_i, y_i, z_i\}$ while they were being searched. The GO would search for the best values of $\{x_i, y_i, z_i\}$ within $[-L/2, L/2]$ by minimizing σ^2 with respect to $\{x_i, y_i, z_i\}$. When the GO iteration was completed, the coordinates of the resultant 'optimized configurations' produced by the Dakota-GMM API were restricted to lie within $[-L/2, L/2]$. It is to be noted that the lower and upper limits for

the GO search need not strictly abide by the above prescription as long as these limits are sufficiently large to cover the smallest and largest coordinates in the ground-truth configuration. Essentially, the limits set in the GO search have to be such that they must cover the smallest and largest values of the coordinates in the ground-truth configuration, so that the resultant optimized configuration was numerically possible to be matched with that from the ground-truth ones, if at all. Having said that the limits must not be excessively large to overburden the global optimization search. An unnecessarily large box size could run into pragmatic issues such as inefficiency and over expensive computational cost in reaching the global optimization goal.

Ideally, σ^2 should be suppressed to as close to zero as possible by setting the iterative loop to run as long as practically feasible. However, in practice, it is only necessary to suppress the MSE to a reasonably low value above zero, say, $\sigma^2_{\text{tol}} \sim 10^{-3}$. Using the MOGA together with the coliny_pattern_search method in a hybrid mode, a typical global optimization search for up to a maximum of 60000 steps would arrive at a value of $\sigma^2 \approx \sigma^2_{\text{tol}}$. In practice, convergence could be achieved much earlier than the maximal step of 60000.

It is possible, if desired, to hit a value of σ^2 lower than σ^2_{tol} if further fine-tuning to the parameters in the GO was pursued. In the present work, a curve reproduction was deemed successful if a completed global optimization search hits an MSE value of less than $\sigma^2_{\text{tol}} = 0.0015$, an arbitrary but reasonable criterion. It was found that, given any arbitrary $\sigma^{\text{mock}}_{\text{ext}}(\lambda)$ curve, a global optimization search did not always successfully return an MSE that fulfills the σ^2_{tol} criteria. Often manual tweaking of the parameters used in the MOGA or coliny_pattern_search algorithms had to be carried out on a case-by-case basis before a successful curve reproduction could be attained for any $\sigma^{\text{mock}}_{\text{ext}}(\lambda)$ curve. The scope of the present work is limited to using only MOGA and coliny_pattern_search methods. Despite the possibility that a highly suppressed MSE could in principle be achieved with other suitable derivative-free global search methods offered in the Dakota package, these options were not explored since the two methods (MOGA and coliny_pattern_search) were sufficient to demonstrate the working principle of the present approach.

2.4. Procedure of Comparison with Ground-Truth Configuration

In the 'comparison with ground-truth configuration' step, the optimized configuration produced by the Dakota (which corresponds to the best σ_{ext} curve overlapping maximally with the mock experimental curve) was retrieved from the output data to quantitatively compare with the ground-truth configuration corresponds to the mock experimental curve. The comparison was quantified in terms of a similarity index (s.i.), s, defined via [21]

$$s = \frac{1}{N}\sum_{i=1}^{N}(k_i+1)^{-1}, \quad k_i = \left|\sqrt{d_{i,1}} - \sqrt{d_{i,0}}\right|, \tag{2}$$

where $d_{i,0}$ and $d_{i,1}$ represent the sorted distance of particles relative to the average positions (center of mass) in the aggregates label '0' and '1', respectively; N corresponds to the number of particles; and the subscript i indexes the particles in the aggregate. Here, '0' is identified as the ground-truth configuration while '1' is the transient configuration generated during the global optimization search. $s \to 0$ means that the two configurations in the comparison have little configurational similarity, while $s \to 1$ infers that the two configurations coincide with each other. Note that the definition of s in Eq. (2) is independent of the orientation of both aggregates '0' and '1' in 3D space.

Upon completion of a successful global optimization search, a set of optimized results were obtained, including a minimized value of the mean square error (MSE) σ^2, an optimized extinction cross-section curve $\sigma_{\text{ext}}(\lambda)$ that maximally coincided with the mock experimental curve $\sigma^{\text{mock}}_{\text{ext}}(\lambda)$, and a corresponding optimized configuration $\{x_i, y_i, z_i\}_{\text{optimized}}$. The MSE σ^2 was pushed below a tolerance of σ^2_{tol}. Visual inspection of the optimized $\sigma_{\text{ext}}(\lambda)$ overlapped with $\sigma^{\text{mock}}_{\text{ext}}(\lambda)$ showed two curves that were maximally coincidental, providing intuitive assurance that the global optimization capability offered by the hybrid MOGA + coliny_pattern_search algorithms (see, for example, plot (a) in Figs. 3–5 in the Results and Discussion section) had successfully minimized σ^2. The optimized $\sigma_{\text{ext}}(\lambda)$ curve was visually inspected alongside $\sigma^{\text{mock}}_{\text{ext}}(\lambda)$, revealing two curves that were highly coincidental. This provided intuitive assurance that the hybrid MOGA + coliny_pattern_search algorithms, which were employed for global

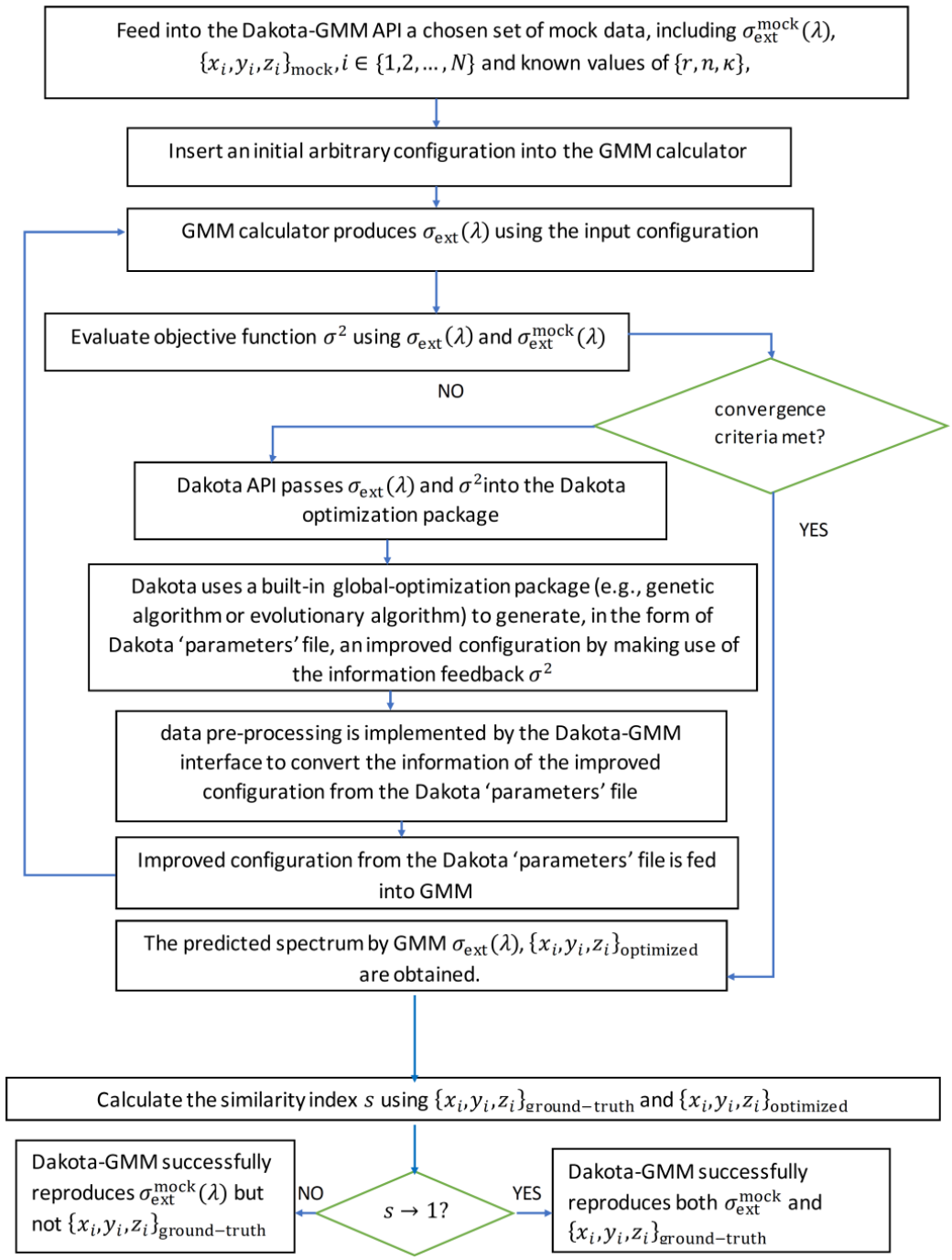

Figure 2. Flowchart of the Dakota-GMM scheme (assuming no manual tweaking of the parameters in the GO are required). This is a more technical version of the flowchart in Fig. 1.

optimization, had effectively minimized σ^2. A sample plot (a) in Figs. 3–5 presented in the Results and Discussion section exemplifies this outcome. The similarity index s was used to measure the difference between $\{x_i, y_i, z_i\}_{\text{optimized}}$ and $\{x_i, y_i, z_i\}_{\text{ground-truth}}$ configurations. Intuitively, a highly suppressed value of σ^2 was expected to correspond to $s \to 1$. A more technical version of the flowchart in Fig. 1 is provided in Fig. 2 to summarize the Dakota-GMM scheme.

Note that r, n, κ, N are all known parameters that were fed into the GMM calculator in the global

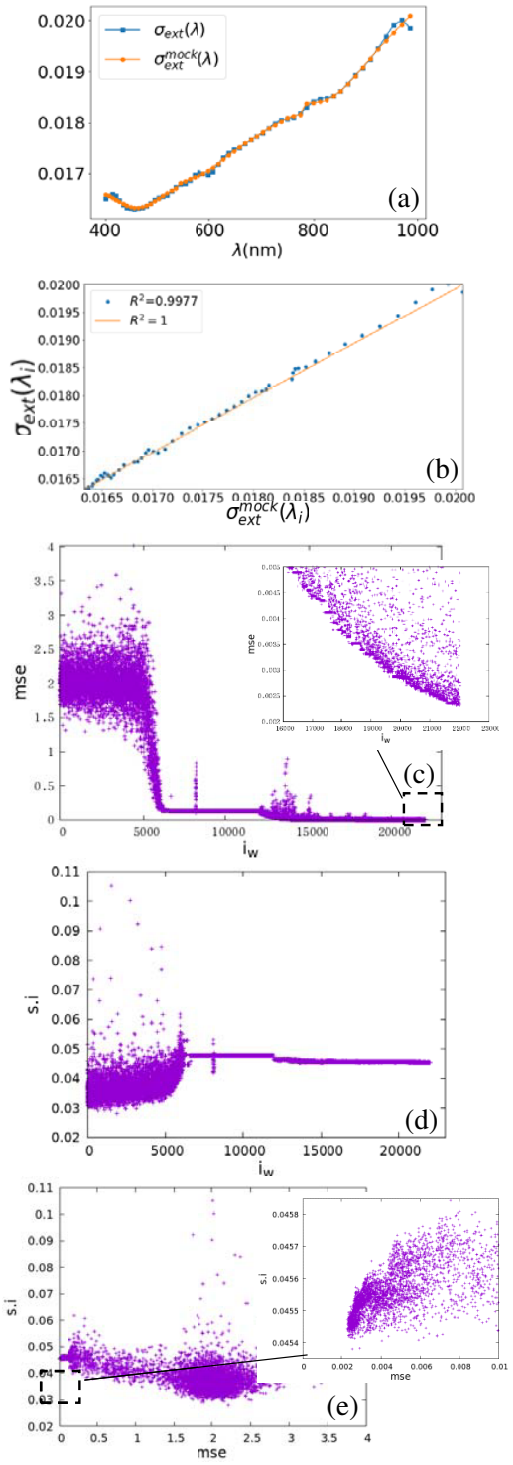

Figure 3. Numerical output for the mock data set 1: $\{r, n, \kappa, N\} = \{125.0, 2.2, 8.5, 26\}$. (a) $\sigma_{\text{ext}}(\lambda)$, $\sigma_{\text{ext}}^{\text{mock}}(\lambda)$ on the same plot. (b) $\sigma_{\text{ext}}(\lambda)$ vs. $\sigma_{\text{ext}}^{\text{mock}}(\lambda)$ at common λ_i. (c) mse vs. i_w. (d) s.i. vs. i_w. (e) s.i. vs. σ^2. The inset in (c) and (e) is a magnification near the minimum of σ^2.

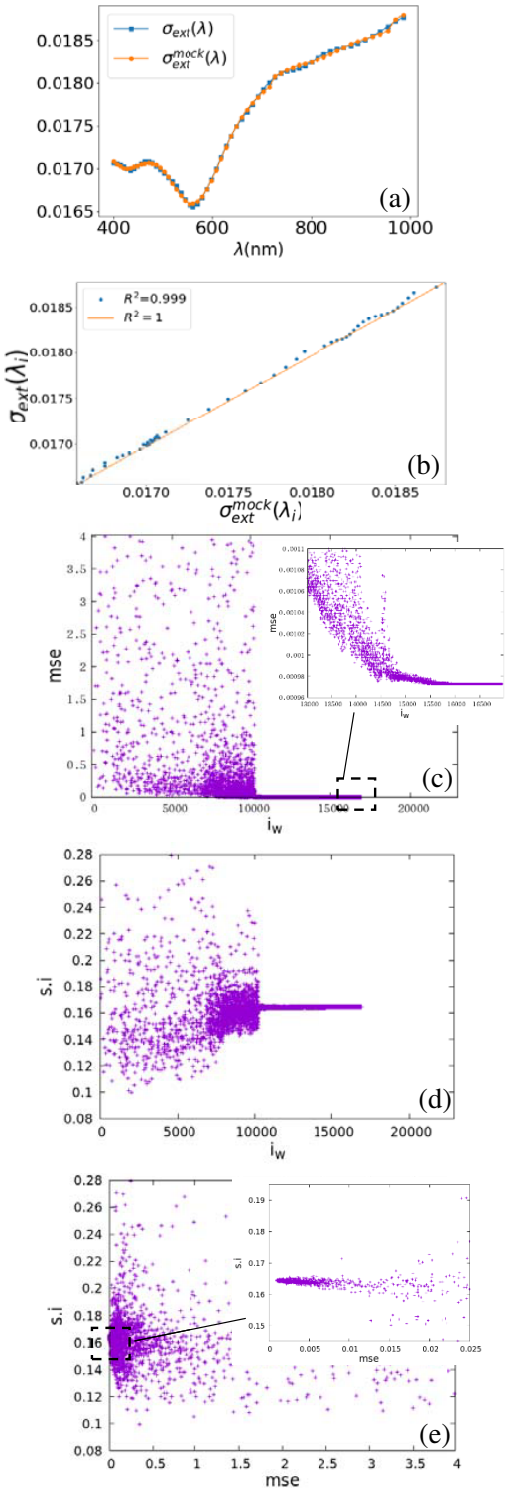

Figure 4. Numerical output for the mock data set 2: $\{r, n, \kappa, N\} = \{225, 1.25, 8.5, 14\}$. (a) $\sigma_{\text{ext}}(\lambda)$, $\sigma_{\text{ext}}^{\text{mock}}(\lambda)$ on the same plot. (b) $\sigma_{\text{ext}}(\lambda)$ vs. $\sigma_{\text{ext}}^{\text{mock}}(\lambda)$ at common λ_i. (c) mse vs. i_w. (d) s.i. vs. i_w. (e) s.i. vs. σ^2. The inset in (c) and (e) is a magnification near the minimum of σ^2.

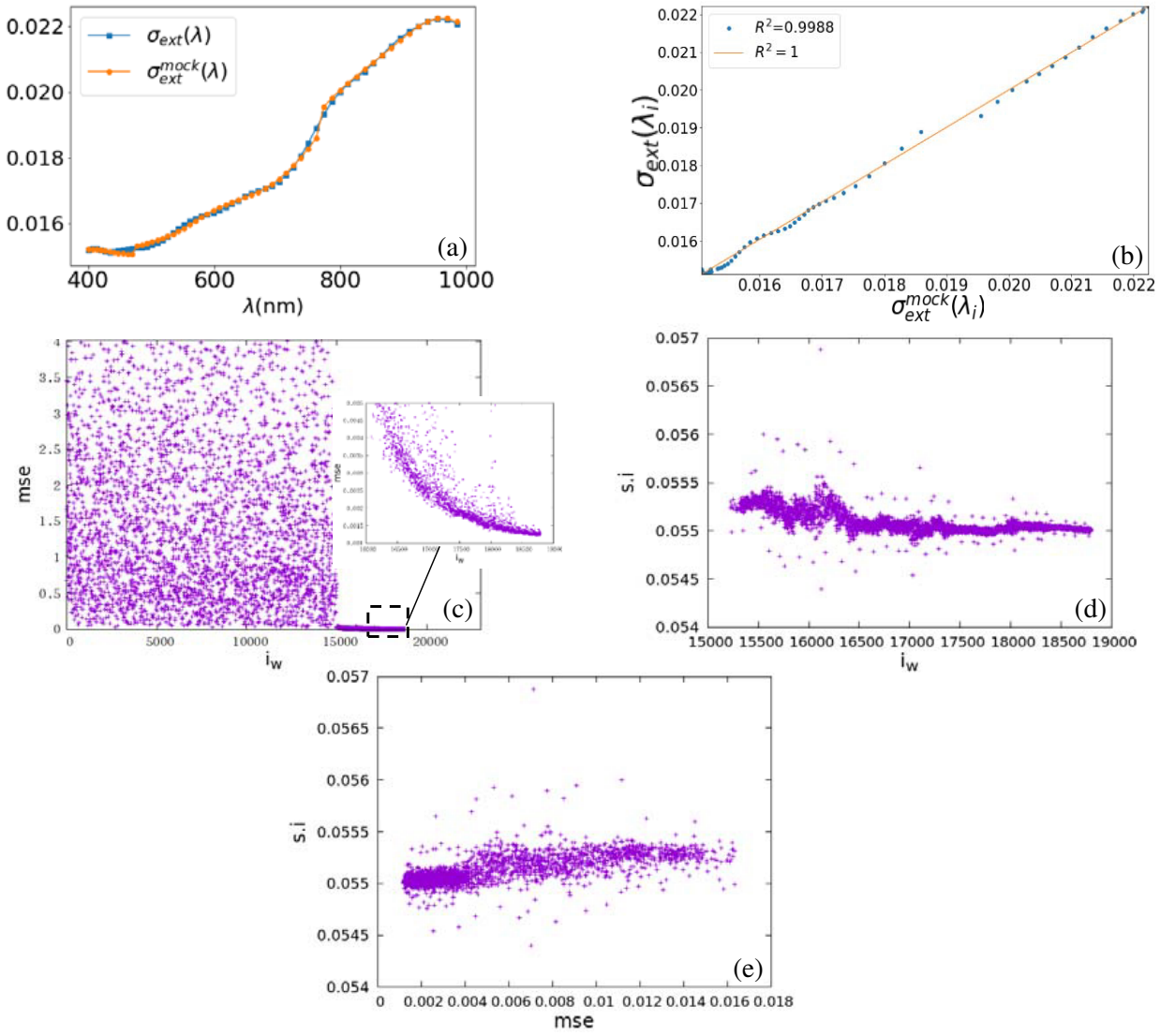

Figure 5. Numerical output for the mock data set 3: $\{r, n, \kappa, N\} = \{75.0, 1.05, 7.5, 18\}$. (a) $\sigma_{\text{ext}}(\lambda)$, $\sigma_{\text{ext}}^{\text{mock}}(\lambda)$ on the same plot. (b) $\sigma_{\text{ext}}(\lambda)$ vs. $\sigma_{\text{ext}}^{\text{mock}}(\lambda)$ at common λ_i. (c) mse vs. i_w. (d) s.i. vs. i_w. (e) s.i. vs. σ^2. The inset in (c) is a magnification of the plot near the minimum of σ^2.

minimization iteration. It is in principle possible to make these four as unknown variables in the global minimization problem. But since we were aiming only to provide a proof of working principle to the Dakota-GMM scheme for solving the specific type of electromagnetic inverse scattering problem, the inclusion of r, n, κ, N as variables to be optimized by the global optimization search were not attempted but postponed to future work.

To concisely explain the entire process of the workflow, we first generated a collection of random N-particle mock aggregates with fixed radius, real, and complex refractive indices. The corresponding extinction cross-section curve $\sigma_{\text{ext}}^{\text{mock}}(\lambda)$ for each mock aggregate was calculated by feeding its configurational and physical parameters into the GMM calculator. We then used the Dakota-GMM API to perform a global optimization, initialized from a random configuration, to search for an optimized trial configuration for which the corresponding objective function σ^2 in Eq. (1) is strongly suppressed to below a preset threshold. If a solution to the global optimization is found, the return consists of two things: (i) An optimized trial curve $\sigma_{\text{ext}}(\lambda)$ that was quantitatively identical to the specific mock curve

used in the definition of σ^2, (ii) the corresponding trial configuration that produces the optimized trial curve. Finally, a similarity index is calculated between the mock and optimized trial configurations (based on Eq. (2)) to determine if their configurations matched with each other.

3. RESULTS AND DISCUSSION

In the present study, a series of optimized results, i.e., $\sigma_{\text{ext}}(\lambda)$, MSE (i.e., σ^2); $\{x_i, y_i, z_i\}_{\text{optimized}}$ and similarity s had been obtained by feeding the Dakota-GMM API with mock data $\sigma_{\text{ext}}^{\text{mock}}(\lambda)$ generated via the mock data generation procedure. The results obtained are presented in this section.

We tested the Dakota-GMM scheme with random configurations containing different numbers of constituent particles N and varying values of $\{r, n, \kappa\}$. We found that successful curve reproduction was always possible with sufficient effort put into tweaking the parameters of the genetic algorithm. To illustrate the working principle, we present three selected random configurations, but many other successful runs shared similar characteristics to these demonstrative cases. We do not show the results from other configurations, as their general characteristics were similar to those presented here. The random mock configurations are characterized by the parameter set 1: $\{r, n, \kappa, N\} = \{125, 2.2, 8.5, 26\}$, set 2: $\{r, n, \kappa, N\} = \{225, 1.25, 8.5, 14\}$, and set 3: $\{r, n, \kappa, N\} = \{75, 1.05, 7.5, 18\}$. For each of these configurations, a set of figures is presented to illustrate the essential features of the output generated by the Dakota-GMM scheme along with the corresponding experimental mock curve. Each figure includes scatter plots labeled as (a), (b), (c), (d), and (e).

(a) The final $\sigma_{\text{ext}}(\lambda)$ curve obtained at the end of the iteration overlaid on the same plot along with the $\sigma_{\text{ext}}^{\text{mock}}(\lambda)$ curve,

(b) $\sigma_{\text{ext}}(\lambda)$ vs. $\sigma_{\text{ext}}^{\text{mock}}(\lambda)$ at each common λ_i,

(c) MSE (i.e., σ^2) vs. i_w. The inset displays the zoom-in version of the mse vs. i_w plot near the minimum of MSE.

(d) Similarity index (i.e., s.i.) vs. i_w,

(e) s.i. vs. mse. The inset displays the zoom-in version of the s.i. vs. MSE plot near the minimum of mse.

i_w refers to the number of steps executed during the optimization search iteration. In Dakota terminology, it is known as 'number of function evaluation'. Figs. 3–5 display these plots for each of these parameter sets.

The (a) and (b) plots in Figs. 3–5 show vividly that the Dakota-GMM had performed an excellent curve reproduction as the mock and Dakota-produced curves coincide to a visually indistinguishable degree. Quantitatively, the suppressed value of MSE listed in each plot labeled (a) is lower than σ_{tol}^2. In plot (b) where the optimized cross-section is plotted vs. the ground-truth cross-section, R-squared, a statistical measure of how close the data are to the fitted regression line, shows $R^2 \approx 1$, inferring that the two plots are numerically similar to each other to a high degree.

The (c) plot in Figs. 3–5 shows that as the search algorithm progressed, MSE would soon pass through a threshold beyond which it is consistently driven into a minimum until it hits the stopping criteria set in the Dakota script. The inset in the (c) plot displays a zoom-in detail of the MSE trajectory near the convergent point. It is observed that the specific behavior of MSE dropping with i_w differs from case to case. A different choice of parameters used in the MOGA-coliny_pattern_search hybrid mode also affected the specific behavior of MSE dropping with i_w. Irrespective of how the MSE dropped and converged, the MOGA and coliny_pattern_search in hybrid mode could always attain the objective to fulfill the MSE tolerance of σ_{tol}^2, provided that sufficient manual tweaking of the parameter-tuning was attempted. There were many instances where the two global optimization algorithms initially failed to obtain a suppressed MSE. However, finally, all such initially stubborn behavior was tamed when sufficient manual effort was made to tweak the parameters. This observation infers that it is generally possible to attain curve reconstruction for any arbitrary mock experimental curve with the Dakota-GMM scheme.

At this juncture, it is appropriate to comment on the feasibility and reliability of the results of the curve reconstruction, as illustrated in plots (a), (b) and (c) in Figs. 3–5. These were obtained as

the solutions to the global optimization of minimizing the objective function, i.e., when the stopping criterion $\sigma^2 < \sigma^2_{\text{tol}}$ was achieved. Regardless of the detailed history of the evaluation of MSE vs. i_w (as shown in the (c) plots in Figs. 3–5), and the random initial configuration from which the search was initiated, the output of the optimization procedure was in the form of an optimized $\sigma_{\text{ext}}(\lambda)$ curve that was approximately identical to the target mock curve, $\sigma^{\text{mock}}_{\text{ext}}(\lambda)$. The target mock curve $\sigma^{\text{mock}}_{\text{ext}}(\lambda)$ was unique for a given curve reconstruction case. In this sense, once the solution of the global optimization was successfully produced at the end of an optimization search, it was unique for that curve reconstruction case, regardless of the initial configuration or the parameters used in the hybrid global optimization algorithm. The uniqueness of the solution to the curve reconstruction problem holds true for any aggregate system, regardless of the variation in the physical parameters. Based on this reasoning, then we can be confident that the solution shown in the illustrative results in plots (a), (b), and (c) in Figs. 3–5 are feasible and reliable.

Plots (d) and (e) in Figs. 3–5 show the s.i. vs. i_w and s.i. vs. MSE scatter plots, respectively. The s.i. data points displayed were obtained via post-processing after the global optimization searches process ended. The value of s.i. was never fed back into the global optimization loop because the ground-truth configuration, which was the information required to calculate s.i., was not supposed to be known by the global optimizer. Plots (d) and (e) reveal an unfortunate finding that despite the Dakota-GMM scheme reproduces the mock experimental curves, it cannot reproduce the ground-truth configuration. Based on the design of the Dakota-GMM scheme, the optimized configuration at the end of the global optimization search, which successfully produces a curve closely similar to the mock experimental curve (with an R-square close to 1), is intuitively expected to be identical to the ground-truth one. However, the trajectory of s.i. displayed by the distribution of the data point in plots (d) shows that during the process of working towards its objective to minimize the objective function (i.e., MSE), the search algorithm causes the generated configurations to get locked into a specific configuration space when i_w proceeds beyond a threshold value indicated by a red arrow in plots (c). At the indicated threshold i_w, an abrupt drop in MSE occurs, indicating that the global search algorithm has zoomed into a restricted region of parameter space to search for a minimized MSE within it. Variation in the configurations generated within the restricted parameter space region beyond the i_w threshold becomes strongly suppressed, resulting in a 'locked' s.i., which is manifested in the form of an approximately constant s.i. line seen in the (d) plots. The restricted region of the parameter space it zooms in contains only the minimum for the MSE but not the ground-truth configuration. The (e) plots provide another perspective of the s.i. trajectory as the MSE is being minimized. It shows that the value of s.i. scatters randomly before the MSE passes the threshold i_w. The (e) plots essentially reveal that a minimized MSE is not correlated with the desired ground-truth configuration (otherwise it would have shown the s.i. tending toward unity as MSE shrinks towards its local minimum). One can envisage a repeated attempt to subject a mock curve for rebooted global optimization searches with a new initial random configuration and random seed value, while the other parameters in the MOGA and coliny_pattern_search are retained. In these rebooted runs, the same 'lock-in' scenario will still occur (but perhaps in a different patch of parameter space). Once a global optimization search experiences a lock-in beyond the threshold i_w, and if the s.i. at the 'entrance' point is much less than unity, the consecutive s.i. will hover around the same entrance value until the end of the search iteration, offering no chance to hop out from the lock-in fate to hit a value of unity in the remaining search steps.

Based on the analysis of the data presented in Figs. 3–5, it is reasonable to conclude that there are possibly many different configurations that could produce a numerically similar curve. In other words, there is a lack of one-to-one correspondence between a curve and the configuration giving rise to it. This situation should be true at least in the scenario where the MSE is only highly suppressed but not exactly zero. At this point, it is not possible to tell whether a one-to-one correspondence between a curve and its corresponding configuration could be established if a vanishing MSE were attained. The hybrid global search algorithms attempted in the present scheme, with the stopping criteria set by σ^2_{tol} appear to unavoidably run into the fate of being trapped in a local minimum.

4. CONCLUSION

To attain the reconstruction of a ground-truth configuration, one necessary requirement is to overcome the local minima trapping issue. To this end, a more sophisticated global optimization searching scheme is called for. It is envisaged that such an advanced search algorithm would hop to a new region in the parameter space after locating a local minimum, in the spirit of 'temperature annealing' [22] or 'basin hopping' [23], to undergo many rounds of strategic search until all local minimum encountered in the entire (or nearly so) parameter space is exhausted. PTMBHGA [24] is one of the many advanced global search algorithms published in the literature. It was used for identifying ground states of atomistic clusters in a highly dimensional and complex potential energy surface (PES) of atomistic interaction potential. Supplanting the global search algorithm with PTMBHGA could be a possible direction for future attempts to fix the local minimum trapping issues encountered in the present Dakota-GMM scheme.

As an independent consideration, there is speculation that incorporating multiple objective functions, in addition to the objective function based on the extinction curve, may help overcome the local minima trapping issue. For example, the GMM could produce other independent optical responses such as scattering and absorption cross-sections, which could be used to define additional objective functions. By making these objectives part of the multiple objectives that the MOGA aims to minimize additional constraints, and discrimination capabilities could be introduced to the global search. This could potentially resolve the problem of many different configurations sharing the same mock curve and improve the search for an optimized configuration.

ACKNOWLEDGMENT

Y. L. Thong acknowledges the support of sponsorship from the Ministry of Education, Government of Malaysia.

REFERENCES

1. Gouesbet, G. and G. Gréhan, *Generalized Lorenz-Mie Theories*, Springer, Berlin, 2011.
2. Mie, G., "Beiträge zur optik trüber medien, speziell kolloidaler metallösungen," *Annalen der Physik*, Vol. 330, 377–445, 1908.
3. Liang, C. and Y. T. Lo, "Scattering by two spheres," *Radio Science*, Vol. 2, 1481–1495, 1967.
4. Bruning, J. and Y. T. Lo, "Multiple scattering of EM waves by spheres. Part I — Multipole expansion and ray-optical solutions," *IEEE Transactions on Antennas and Propagation*, Vol. 19, 378–390, 1971.
5. Mackowski, D. W., "Analysis of radiative scattering for multiple sphere configurations," *Proceedings of the Royal Society of London Series A: Mathematical and Physical Sciences*, Vol. 433, 599–614, 1991.
6. Mackowski, D. W. and M. I. Mishchenko, "Calculation of the T matrix and the scattering matrix for ensembles of spheres," *JOSA A*, Vol. 13, 2266–2278, 1996.
7. Xu, Y.-L. and B. Å. S. Gustafson, "A generalized multiparticle Mie-solution: Further experimental verification," *Journal of Quantitative Spectroscopy and Radiative Transfer*, Vol. 70, 395–419, 2001.
8. Xu, Y.-L. and B. Å. S. Gustafson, "Experimental and theoretical results of light scattering by aggregates of spheres," *Applied Optics*, Vol. 36, 8026–8030, 1997.
9. Xu, Y.-L., "Electromagnetic scattering by an aggregate of spheres: Asymmetry parameter," *Physics Letters A*, Vol. 249, 30–36, 1998.
10. Xu, Y.-L., "Electromagnetic scattering by an aggregate of spheres: Errata," *Applied Optics*, Vol. 37, 6494, 1998.
11. Xu, Y.-L. and R. T. Wang, "Electromagnetic scattering by an aggregate of spheres: Theoretical and experimental study of the amplitude scattering matrix," *Physical Review E*, Vol. 58, 3931–3948, 1998.

12. Xu, Y.-L., "Efficient evaluation of vector translation coefficients in multiparticle light-scattering theories," *Journal of Computational Physics*, Vol. 139, 137–165, 1998.
13. Xu, Y.-L., B. Å. S. Gustafson, F. Giovane, J. Blum, and S. Tehranian, "Calculation of the heat-source function in photophoresis of aggregated spheres," *Physical Review E*, Vol. 60, 2347–2365, 1999.
14. Jia, R., X. Zhang, F. Cui, G. Chen, H. Li, H. Peng, and S. Pei, "Machine-learning-based computationally efficient particle size distribution retrieval from bulk optical properties," *Applied Optics*, Vol. 59, 7284–7291, 2020.
15. Mitchell, M., *An Introduction to Genetic Algorithms*, MIT Press, 1998.
16. Goldberg, D. E., *Genetic Algorithms in Search, Optimization, and Machine Learning*, 989, Addison-Wessley Publishing Co., Inc., MA, 1989.
17. Adams, B. M., W. J. Bohnhoff, K. R. Dalbey, et al., "Dakota, a multilevel parallel object-oriented framework for design optimization, parameter estimation, uncertainty quantification, and sensitivity analysis: Version 6.15 user's manual," *Sandia Technical Report SAND2020-12495*, November 2021.
18. Murata, T. and H. Ishibuchi, "MOGA: Multi-objective genetic algorithms," *Proceedings of 1995 IEEE International Conference on Evolutionary Computation*, Vol. 1, 289, 1995.
19. Eddy, J. and K. Lewis, "Effective generation of pareto sets using genetic programming," *Proceedings of the ASME 2001 International Design Engineering Technical Conferences and Computers and Information in Engineering Conference*, Vol. 2B, 783–791, 2001.
20. Eddy, J., "JEGA V 2.3. computer software," USDOE, https://www.osti.gov//servlets/purl/1231173, Mar. 25, 2009.
21. Ng, W. C., T. L. Lim, and T. L. Yoon, "Investigation of melting dynamics of Hafnium clusters," *Journal of Chemical Information and Modeling*, Vol. 57, 517–528, 2017.
22. Ingber, L., "Simulated annealing: Practice versus theory," *Mathematical and Computer Modelling*, Vol. 18, 29–57, 1993.
23. Wales, D. J. and J. P. K. Doye, "Global optimization by basin-hopping and the lowest energy structures of Lennard-Jones clusters containing up to 110 atoms," *J. Phys. Chem. A*, Vol. 101, 5111–5116, 1997.
24. Hsu, P. J. and S. K. Lai, "Structures of bimetallic clusters," *The Journal of Chemical Physics*, Vol. 124, 044711, 2006.